ACCEPTED MANUSCRIPT • OPEN ACCESS

Exploring the effects of ambient conditions on the cryogenic cooling times of offshore structures: Towards optimising sustainability and the decommissioning timescale

To cite this article before publication: Kenneth Bisgaard Christensen *et al* 2024 *Sustain. Sci. Technol.* in press https://doi.org/10.1088/2977-3504/ad8d60

IOP Publishing Journal Title
Journal **XX** (XXXX) XXXXXX https://doi.org/XXXX/XXXX

Exploring the Effects of Ambient Conditions on the Cryogenic Cooling Times of Offshore Structures: Towards Optimising Sustainability and the Decommissioning Timescale

Kenneth Bisgaard Christensen[1,2], Alireza Maheri[1] and M. Amir Saddiq[1]

[1] School of Engineering, University of Aberdeen, King's College, Old Aberdeen, United Kingdom
[2] School of Physics and Astronomy, University of Manchester, Manchester, United Kingdom

E-mail: kenneth.bisgaard@physics.org

Received xxxxxx
Accepted for publication xxxxxx
Published xxxxxx

Abstract

This study investigates the influence of ambient conditions on cryogenic cooling times for medium-carbon steel-grade ISO EN 1.0456 (ASTM A333 Gr.6) processing pipes, focusing on the air velocity, ambient temperature, and cooling medium. Using MATLAB, baseline cooling times were computed for air velocities of 0–25 m s−1, considering both in-air cooling and saltwater environments. At a target temperature of −50 °C, which is critical for achieving specific impact energy absorption (E_i), the cooling times increased due to varying heat transfer coefficients influenced by the air velocity. Pipe wall thicknesses of 12.7 and 25.4 mm resulted in 5.7 and 6.9% increases in the cooling time, respectively. The viability of cryogenic conditions was validated for low-energy fracturing in carbon steel, utilising the MATLAB finite difference method model to simulate transient heat transfer. The impact of temperature on E_i was evaluated, and the efficiency of the proposed cryogenic cooling and cutting system was explored, incorporating factors such as air velocity and temperature. The importance of insulating effects in real-world applications was highlighted based on results obtained for the insulating residues. Validation against commercial finite element method software confirmed the accuracy of the numerical model, suggesting the broad applicability of these findings across carbon steel families. The critical role of the surface area in determining the cooling efficiency is also identified, and the trade-off between enhanced cooling, the internal surface area, costs, and energy consumption are discussed to advocate for a balanced approach. This research contributes to Sustainable Development Goals 9 (Industry, Innovation, and Infrastructure), 13 (Climate Action), and 14 (Life Bellow Water) by proposing an innovative and environmentally friendly cryogenic cooling technology to optimise the decommissioning of offshore structures. Overall, this study lays the groundwork for understanding the intricacies of cryogenic cooling to foster more sustainable and efficient manufacturing processes.

Word count: 5,955 words, excluding references.

Keywords: Cryogenic cooling, Carbon steel, Heat transfer, Embrittlement, Finite Difference Method, A333

IOP Publishing Journal Title
Journal **XX** (XXXX) XXXXXX https://doi.org/XXXX/XXXX

Nomenclature:

Atmospheric pressure	ATM
Cryogenic cooling and cutting system	CCCS
Degrees Celsius	°C
Density	ρ
Dimensional grid size	Δx/Δy
Heat transfer coefficient	H_x
Impact energy absorption	E_i
Kelvin	K
Shear modulus	G
Shear strength	σ
Shear stress	τ
Standard temperature and pressure	STP
Specific heat capacity	C_p
Temperature difference	ΔT
Thermal conductivity	λ
Outer diameter	D_O
Wall thickness	W_t

1. Introduction

In the coming decades, thousands of offshore oil and gas structures worldwide will become obsolete and require decommissioning. However, current removal methods often fail to achieve optimal environmental, societal, and economic outcomes [1,2]. It is therefore crucial to evaluate decommissioning options based on environmental, financial, socioeconomic, and health and safety criteria. Previous research has demonstrated that ecosystem functions and services tend to improve as these structures age and vary geographically, emphasising the importance of an ecosystem-based approach in decommissioning decisions. A comparative assessment of material, energy, and financial flows for various decommissioning scenarios, including the removal of large steel topsides and jackets, and their environmental impacts, is therefore necessary [3,4].

Despite the rigorous safety designs of offshore structures, their prolonged lifespans expose them to potential damage from factors such as collisions, explosions, corrosion, fatigue, and overloading. Predicting the initiation and propagation of fractures in these structures is a formidable challenge [5,6], especially considering the role of such factors in determining the necessary cutting time for repair or decommissioning [7,8]. In the North Sea Region, covering an area of approximately ~1119 km², decisions regarding the decommissioning or in-situ preservation of pipelines during their end-of-life cycles require meticulous consideration.

Unfortunately, current data related to the environmental impacts of these alternatives are not readily available. In particular, for pipelines with an outer diameter (D_O) >762 mm (30 in), it is imperative to reclaim ≥50% of the seabed occupied by these structures. However, the safe and cost-effective removal of pipelines with a D_O >406 mm (16 in) has not been tested on a large scale, thereby exposing a technological gap and underlining the intricacies of the considerable piping infrastructure found in the North Sea Region [9,10]. An alternative approach wherein the cutting ability is unaffected by the pipe D_O is therefore required to bridge the technological gap in the decommissioning process [11]. In the dynamic realm of offshore platform decommissioning, the intricate interplay between the effects and techniques, coupled with a conscientious consideration of environmental aspects and management strategies, has emerged as a central focus for scientific advancement. Key dimensions that are known to influence offshore decommissioning, including environmental considerations and management practices, assume pivotal roles, and their significance is contingent on specific platform characteristics, such as the type and location [2]. However, the decision-making process for the decommissioning of offshore platforms remains intertwined with uncertainties arising from hydrocarbon prices, maintenance costs, environmental impact, structural capacities, and deterioration [10]. Among these parameters, the integration of advanced technologies has emerged as a crucial factor for optimising efficiency and mitigating environmental impacts [2,12]. With an estimated 2000 offshore platforms worldwide slated for decommissioning by 2040, this complex undertaking is not only financially demanding, but also necessitates rigorous adherence to national and international laws and regulations aimed at safeguarding the environment. As such, this process

demands innovative technological solutions for offshore decommissioning [10,12]. To date, scientific investigations in this field have spanned a spectrum of themes, encompassing the development of mathematical models for decision support, environmental impact analyses, criteria for selecting decommissioning options, reviews of decision support tools, and rankings of decommissioning alternatives. A leading force in this evolving landscape is the development of innovative technological solutions to facilitate the decommissioning process [9,10,12]. In general, this dynamic landscape calls for further exploration of novel cutting solutions to promote more sustainable offshore decommissioning practices [13,14]. The effects of the ambient environment on the cooling time of carbon steel for low-energy fracturing [15] is of particular research interest, with alternatives being required to the current cutting techniques, wherein abrasive water jet (AWJ) cutting is especially prevalent in offshore structure decommissioning [16,17]. However, the current process for offshore decommissioning is both slow and time-consuming [18]. Thus, given the anticipated rise in demand for these services over the coming decade, the development of a quicker and more cost-effective cutting method could significantly benefit the industry. Developing such techniques is crucial as it can lead to more efficient project completion and potentially lower environmental [8,16]. Such improvements could also drive down costs and increase the feasibilities of decommissioning projects that are currently considered unviable due to technological and financial constraints.

In alignment with the UN Sustainable Development Goals, particularly SDG 9 (Industry, Innovation, and Infrastructure), SDG 13 (Climate Action), and SDG 14 (Life Below Water), the current study aims to demonstrate the effects of ambient conditions on the cooling times of different carbon steel grades, specifically in the case of the EN1.0456 specimen (ASTM A333 Gr.6), wherein a novel cryogenic cooling and cutting system (CCCS) is proposed. Firstly, ductile-to-brittle transition temperature (DBTT) is investigated to understand this phenomenon in carbon steel at sub-zero temperatures. In addition, a finite difference method model (FDM-M) is created in MATLAB to simulate the transient heat transfer (THT) process for different carbon steel grades. Subsequently, the effects of the ambient temperature on the energy absorption (E_i) in carbon steel are evaluated in the context of low-energy fracturing. Furthermore, the cryogenic cooling required by the CCCS cutting process is investigated by applying a coolant to the surface of the carbon steel geometry. For example, using liquid nitrogen (LN_2) as a cooling medium, its working fluid properties are examined considering the temperature and heat transfer coefficient, while the impact of this coolant on the energy absorption and cooling time of carbon steel is investigated [19,20,21,22]. Moreover, a range of ambient conditions are considered, including air velocity, ambient air temperature, and cooling medium, to determine their effects on the cooling time in an air-cooling environment. Additionally, the effects of insulating residues (e.g., crude oil sludge) on the CCCS cooling process within the processing pipes are determined, and the cooling time and impact energy absorption are calculated to investigate the effects of the fracture zone surface area and geometry on the cooling time. Finally, the ANSYS Workbench and MATLAB platforms are employed to validate the accuracy of the cooling-time calculations and simulations, thereby ensuring the effectiveness of the developed FDM-M. Overall, it is expected that this study will establish a foundation for understanding the cooling time required by CCCS by employing LN_2 as a coolant with specific parameters unique to the harsh North Sea Region (NSR) environment.

2. Materials and Methods

2.1 General considerations

The steel grade material assessed by the numerical models herein was a carbon steel grade known as ISO EN1.0456 (ASTM A333 Gr.6), which has a body centred cubic (BCC) structure (Phelps, 2019). This steel grade was applied for all simulations and calculations to determine the effects of the ambient conditions on the cooling time within the cooling zone of the carbon steel object. LN_2 was employed as the cryogenic cooling agent to reach the desired E_i values for the simulations and calculations. The heat transfer coefficient (h) for LN_2 was set to 128 $\frac{W}{m^2K}$ [21,24,25] to reduce the impact energy absorption capacity of the carbon steel geometry and minimise energy usage in the CCCS fracturing process [6,26,27]. Unless otherwise stated, the ambient conditions employed in this current study were assumed to be standard temperature and pressure (STP), i.e., 293 K (20 °C) and 1 ATM (1013 MPa), which corresponds to an LN_2 working temperature of 77 K (−196 °C) [21,28,29].

All observations were based on calculations and simulations performed in MATLAB by applying the finite difference method (FDM) model designed for this purpose. The FDM model can easily be modified to accommodate the grade of steel, but for the purpose of this study, the medium-carbon steel ISO EN1.0456 (ASTM A333 Gr.6) grade was selected. The chemical elemental composition of the steel specimen is presented in Table 1, whilst its mechanical and thermophysical properties are given in Table 2.

Table *1*: Elemental composition of the ISO EN 1.0456 (ASTM A333 Gr.6) medium-carbon steel [29,32,33].

Iron (Fe)	Carbon (C)	Manganese (Mn)	Phosphorus (P)	Sulfur (S)	Silicon (Si)
≥98.5	≤0.30	≤1.05	≤0.025	≤0.025	≥0.10

Table 2: Mechanical and thermophysical properties of ISO EN 1.0456 (ASTM A333 Gr.6) medium-carbon steel [29,32,33].

Property	Value
Thermal Conductivity (γ)	48 W/m·K
Density (ρ)	7850 kg/m^3
Specific Heat Capacity (c_p)	470 J/kg·K
Young's Modulus	210 GPa
Poisson's Ratio	0.29
Shear Modulus (G)	73 GPa
Shear Strength (σ)	240 MPa
Shear Stress (τ)	30 MPa
Ultimate Tensile Strength (UTS)	415 MPa

The impact energy absorption (E_i) values of the DBTT phase-shifting graphs of three different carbon steel grades are shown in Figure 1 [31], wherein E_i is plotted as a function of temperature; the blue plot corresponds to the ISO EN1.0456 (ASTM A333 Gr.6) specimen employed in the current study, which has a relatively low carbon content of ≤0.03% [30,32,33,35]. The DBTT impact energy absorption curves were obtained by calculating the drop in E_i against the core temperature of the carbon steel specimens using Equation 1:

$$\Delta T_k = \alpha_k + \beta_k \tan(h) \left[\frac{x+c_k}{\delta_k}\right] \quad (1)$$

where ΔT_k represents the change in a material property such as toughness in relation to temperature, α_k is a constant that sets the baseline of the curve, shifting it vertically to match empirical data. β_k is a scaling factor that adjusts the amplitude of the property change across different temperatures. The hyperbolic tangent function, tan(h), provides a smooth, S-shaped transition, ideal for modelling phenomena such as the ductile-to-brittle transition of a material, wherein the property shifts sharply at certain temperatures. In the above equation, x denotes the temperature, c_k represents the position of this sharp transition along the temperature axis, and δ_k is the steepness of the curve, indicating how abruptly or gradually the material properties change with temperature. These data were collected from standards (e.g., ASTM A333/A333M-16), from the standard specifications of seamless and welded steel pipes for low-temperature operations, and from specifications employed in other applications requiring a high notch toughness [33].

As can be seen from Figure 1, the BCC structure and low carbon content of this specimen render it highly susceptible to embrittlement at low temperatures. In addition, it can be seen that the ISO EN1.0456 (ASTM A333 Gr.6) specimen possesses an E_i value of 15 J/cm^2, at approximately −50 °C. This result was derived from the V-notch test data presented in the literature [33,36].

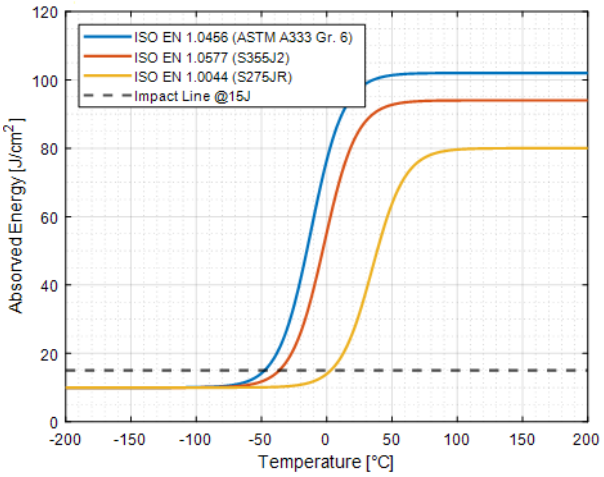

Figure 1. Ductile-to-brittle transitional phase diagram of the ISO EN 1.0xxx medium-carbon steel grades upon variation in temperature [31].

The newly developed MATLAB FDM-M was applied to estimate the cooling times of different grades of carbon steel, depending on their wall thickness (W_t) and the surrounding ambient conditions, as shown in Figure 2. The FDM-M was set up such that there was a difference in ambient conditions between the two sides of the carbon steel object, with external ambient conditions being experienced by the outer side, and internal ambient conditions being experienced by the inside, as illustrated in Figure 2.

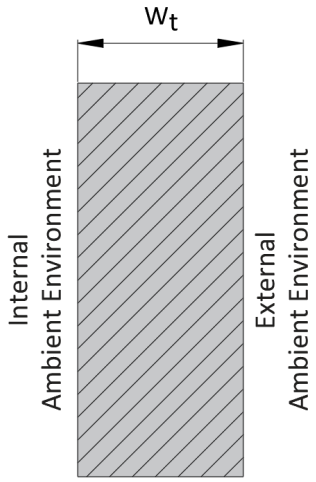

Figure 2. Schematic representation of the two-dimensional cross-section of the carbon steel specimen and the surrounding ambient conditions.

During the cryogenic cooling process, four different sets of external ambient conditions were considered, namely in-air cooling, water cooling (e.g., submersion in saline seawater for offshore structures), natural insulation (e.g., cooling within saline-saturated mud from the seabed or using dry bedrock from the land), and the use of an artificial insulation layer. Figure 3 shows the average heat transfer coefficients under the three most common conditions, which were investigated to determine their effects on the specimen cooling times.

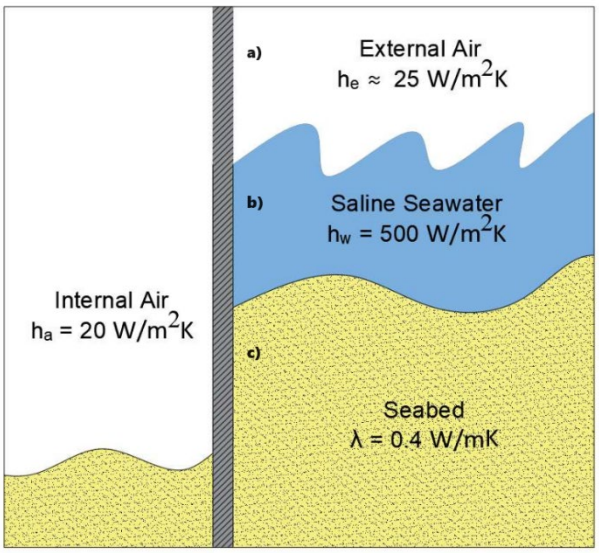

Figure 3. Ambient conditions investigated in the current study: a) External air, b) saline seawater, and c) bedrock from the seabed.

The influence of the ambient air velocity (m s−1) on the convective heat transfer coefficient (h) was examined and the results are presented in Figure 4. This figure was modelled using Equation 2, which is an optimised empirical equation based on an approximation equation for an ambient air velocity (v, m s−1) of 2–25 m s−1 (Engineering Toolbox, 2022).

$$h = 0.25 - 1.1v + 12v^{1/2} \quad (2)$$

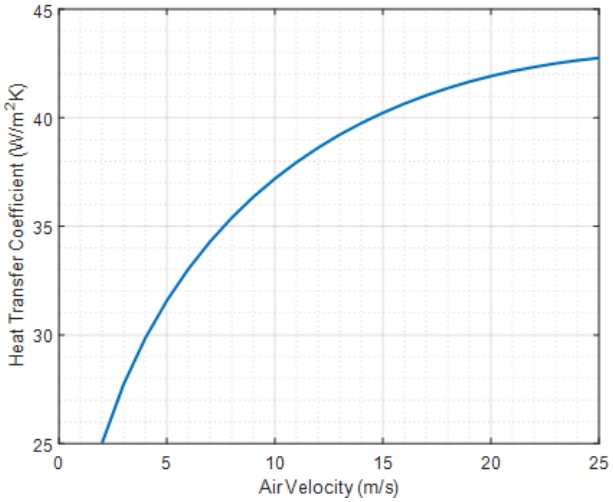

Figure 4. Dependence of the convective heat transfer coefficient of air on the ambient air velocity.

2.2 Numerical simulation methodology

This theoretical study is based entirely on numerical simulations, with no experimental work being conducted. All findings were derived from a finite difference method model (FDM-M) developed in MATLAB, which was employed to simulate the transient heat transfer processes under cryogenic cooling conditions. The accuracy of the FDM-M model was validated through comparison with commercial finite element method (FEM) software (ANSYS Workbench). These simulations allowed for the precise control of variables such as the air velocity, ambient temperature, and cooling medium, thereby enabling a comprehensive investigation of their effects on the cooling times of medium-carbon steel (ISO EN 1.0456, ASTM A333 Gr.6). The results presented reflect the simulated environment and should be interpreted within this computational framework.

The theoretical numerical experiments employed to determine the effects of the ambient conditions on the cooling time of the ISO EN 1.0456 (ASTM A333 Gr.6) medium-carbon steel fracture zone were based on a newly developed MATLAB FDM-M that applied finite difference calculations [38]. To analyse the THT calculations and simulations, MATLAB FDM-M was used to simulate the cooling time and heat distribution within the two-dimensional (2D) cross-section of the medium-carbon steel-grade geometry. MATLAB FDM-M was set up using a range of ambient parameters of STP to calculate the cooling times resulting

from any specific set of ambient conditions. The newly developed MATLAB FDM-M was then applied to calculate the cooling time with a high level of accuracy for various carbon-based steel grades due to their susceptibility to undergo DBTT phase shifting at low temperatures [31].

2.3 Numerical model for the ambient heat transfer calculations

The newly developed MATLAB FDM-M was applied to define the cooling time required for the medium-carbon steel specimen (ISO EN 1.0456, ASTM A333 Gr.6) under different ambient and boundary conditions. This approach was based on the standard set of finite difference equations (T_n^{i+1}). In Figure 5, the cooling element is depicted in blue and corresponds to the LN_2-flooded area of the CCCS, which is in contact with the external environment. The grid layout of the applied 2D FDM equation used to determine the cooling time required to reach −50 °C at the control point (T7) is also shown in Figure 5, wherein the parameters and set-up applied to run the FDM-M calculations are provided.

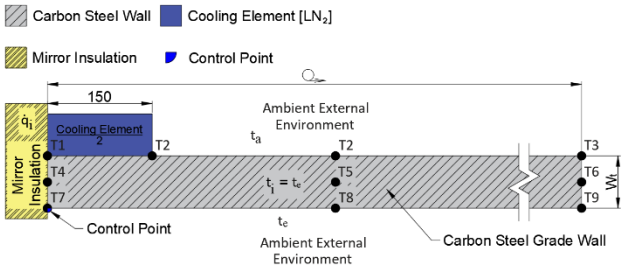

Figure 5. Applied 2D finite difference method (FDM) equation grid layout for the cross-sectional surface of the medium-carbon steel geometry with a defined control point.

3 Results

3.1 Ambient heat transfer calculations

A theoretical study was initially carried out to evaluate the effects of different ambient conditions on the cooling time of a medium-carbon steel specimen required to reach a specific E_i in its fracture zone. Using medium-carbon steel of ISO EN 1.0456 (ASTM A333 Gr.6) grade, the effects of air and water cooling were evaluated at different velocities and temperatures. In addition, the use of insulated cooling (bedrock), where only temperature is a key parameter, was also examined. The in-air cooling time of this medium-carbon steel was found to be influenced by both the air velocity and the ambient air temperature. Therefore, MATLAB FDM-M calculations were used to determine the cooling times required under different air velocities, and to investigate the feasibility of calculating the cooling times for the extra strong (XS) and double extra strong (XXS) specimens (ASTM International, 2004), which are defined in Table 3. It is important to note that the heat transfer coefficient value of ambient air varies depending on specific conditions, such as changes in the ambient air velocity over time. However, for the baseline cooling time FDM-M calculations carried out in MATLAB, the ambient air velocity was assumed to be constant, but was varied from 0 to m s^{-1} at intervals of 2.5 m s^{-1}.

Table 3. W_t sizes for the XS and XXS pipe IDs, as defined by ASTM International, 2004 [38] and (Arntsen, 2020) [29]

Identification (ID)	W_t Size
XS	12.7 mm (0.50")
XXS	25.4 mm (1.00")

3.2 Ambient Heat Transfer Calculations

In addition, the effect of h_a on NSR saline water was evaluated in the contexts of cutting within the sea and in the bedrock below the mudline of the sea floor. The overall cooling time required for the medium-carbon steel specimen to reach a temperature of −50 °C and an E_i point of 15 J/cm^2 within the fracture area of the processing pipes was evaluated [40]. Figure 6 shows the effects of the ambient air velocity on the heat transfer coefficient and the required cooling times for the XS and XXS medium-carbon steel processing pipes. It can be seen that in still air (v = 0 m s−1), the heat transfer coefficient is defined as 320$\frac{W}{m^2K}$, while the maximum cutting operational ambient air velocity of 25 m s−1 gave a heat transfer coefficient of ~41 $\frac{W}{m^2K}$. Using the newly developed FDM-M, theoretical measurements were carried out at ambient air velocity intervals of 2.5 m s−1 (0–25 m s−1) to calculate the cooling time required to reach −50 °C at the cooling point at the bottom surface of the medium-carbon steel specimen. These calculations were carried out for the XS and XXS specimens, and it was found that the required cooling time increased from 193 to 204 s for the XS sample and from 363 to 388 s for the XXS sample, which represent 5.7 and 6.9% increases in the required cooling time upon increasing the air velocity from 0 to 25 m s−1. These results suggest that the ambient air velocity does not have a great impact on the overall cooling time of the medium-carbon steel specimen.

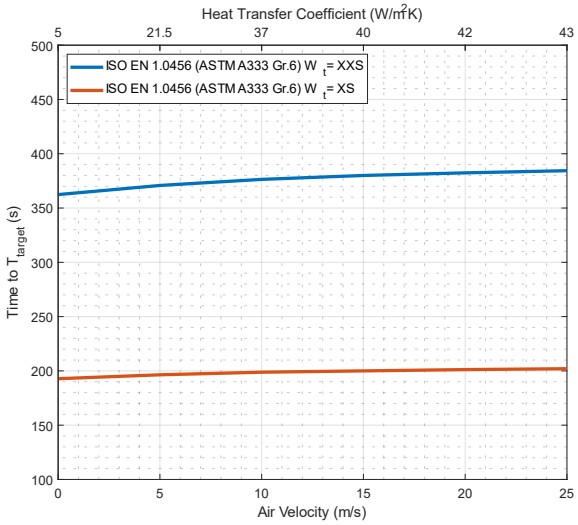

Figure 6. Effect of the air velocity on the transient heat transfer cooling time for the XS and XXS processing pipe specimens.

Figure 7 highlights the significant effect of the air temperature on the cooling time, showing a much greater influence compared to that of the air velocity. As the air temperature was increased from −10 to 30 °C, the cooling time rose from 114 to 220 s for the XS specimen and from 204 to 420 s for the XXS specimen, representing increases of 93 and 106%, respectively. By comparison, the cooling time increased by only 11 s for the XS specimen and 25 s for the XXS specimen with each 2.5 m s−1 increment in air velocity. These results clearly demonstrate that while the air velocity has some impact on cooling, the ambient air temperature plays a far more dominant role in determining the cooling efficiency.

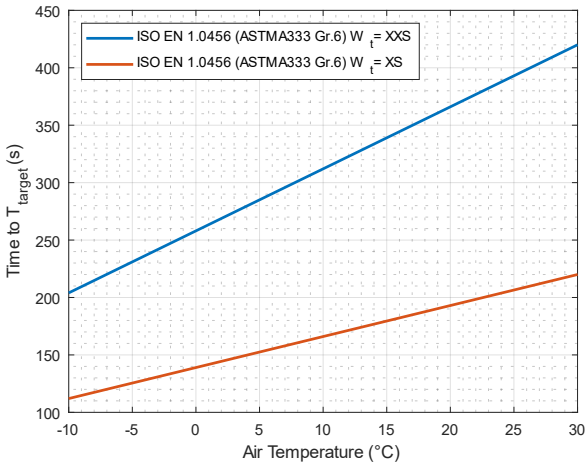

Figure 7. Effect of the air temperature on the transient heat transfer cooling time for the XS and XXS processing pipe specimens.

Subsequently, the cooling time resulting from the use of the LN_2 cryogenic coolant was investigated for the medium-carbon steel processing pipes. As shown in Figure 8, it was found that the time required to cool the XXS pipe fracture area to the desired E_i point of 15 J/cm^2 (i.e., at −50 °C) ranged from 114 s for a heat transfer coefficient of 20 $\frac{W}{m^2K}$, an air velocity of 0 m s−1, and an ambient air temperature of −10 °C, to a time of 233 s for a heat transfer coefficient ~41 $\frac{W}{m^2K}$, an air velocity of 25 m s−1, and an ambient air temperature of 30 °C. For the XS specimen, a lower cooling time limit of 204 s and an upper cooling time limit of 456 s were recorded under the same parameters.

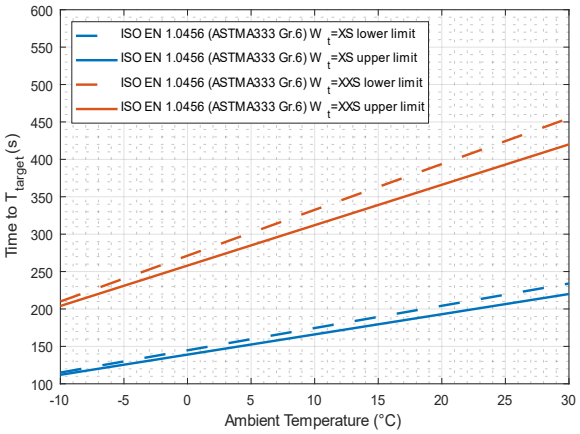

Figure 8. Lower and upper limits for the transient heat transfer cooling times of the XS and XXS processing pipes.

Subsequently, the effects of insulating residues inside the XXS processing pipes (e.g., from crude oil slack), were evaluated using the developed MATLAB FDM-M, as presented in Figure 9. It can be seen that the cooling time was reduced from 456 s (for the clean processing pipe) to 394 s (for the insulated dirty processing pipe), which represents a reduction of 13.6% under the most extreme ambient environmental conditions, with a temperature of −10 °C, an air velocity of 25 m s−1, and at 1 ATM pressure.

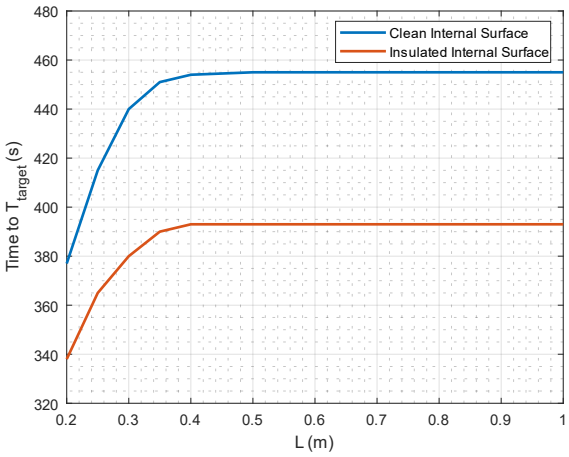

Figure 9. Effect of the internal surface length on the transient heat transfer cooling times of clean and dirty (insulated) XXS processing pipes.

For cutting below the sea level in the saline seawater environment of the NSR, both external and internal cutting processes must be considered. Thus, calculations were carried out for both the XS and XXS medium-carbon steel processing pipes based on conditions under the waterline. Considering the high heat transfer coefficient of the seawater (~500 $\frac{W}{m^2K}$, see Figure 3), heat extraction (h_w) from the water is extremely efficient, so the CCCS cooling process becomes insufficient. As a result, the target temperature of −50 °C cannot be reached within a reasonable maximum timeframe of 7200 s, as defined by the maximum allowed cooling time in the MATLAB FDM-M. In addition, due to this high average heat transfer coefficient of seawater, the cross-sectional surface of the steel wall cooling area of any specific medium-carbon steel grade is so inefficient that it cannot reach the sub-zero target temperature of −50 °C in any given timeframe without the inclusion of an insulating layer between the saline environment and the cooling area of the medium-carbon steel grade. Therefore, only baseline data were collected from the FDM-M calculations, which are not applicable for further investigations into cooling processes of different medium-carbon steel grades.

Finally, the cooling times were investigated for the medium-carbon steel processing pipes within a saturated mud compound of the bedrock below the seabed mudline. During cooling under such conditions, the saturated mud acts as an insulator between the saltwater and the fracture area of the cooling zone. As stated above, such a barrier is required to insulate the cooling zone when LN_2 is used as the cooling agent. The presence of this insulating barrier allows cooling of the medium-carbon steel wall to the required −50 °C and the desired E_i point of 15 J/cm^2. The insulating effect of the saturated mud compound leads to an average thermal conductivity (λ) of 0.2–0.4$\frac{W}{mK}$, thereby allowing cooling by LN_2 to take place in this environment. As a result, the desired level of cooling was achieved in the XS and XXS specimens within 162 and 294 s, respectively, as presented in Figure 10.

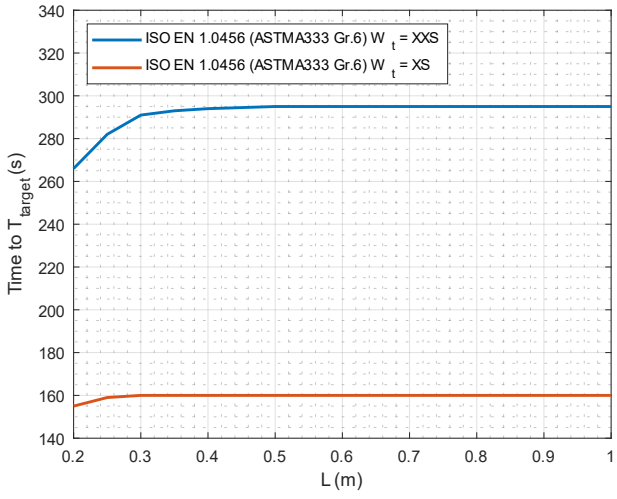

Figure 10. Effect of the internal surface length on the transient heat transfer cooling times of the insulated XS and XXS processing pipes.

3.2 Validation of the MATLAB FDM-M compared to the commercial FEM

To validate the newly developed MATLAB FDM-M for transient heat transfer analysis, a comparison was carried out using a range of widely used numerical techniques for solving partial differential equations (PDEs). This comparison involved both the FDM and the finite element method (FEM), focusing on a medium-carbon steel wall of ISO EN 1.0456 (ASTM A333 Gr.6) grade, with a W_t of 100 mm, a $D_O \leq 10$ m, and a varying cooling bandwidth between 150 and 500 nm.

The FDM-M, which is foundational to MATLAB FDM-M, discretises the 2D geometry into finite-sized cells, approximating the temperatures at each cell based on neighbouring values. It solves the heat transfer equation numerically for each time step; however, its accuracy may be influenced by the grid cell size, potentially causing oscillations. On the other hand, the FEM divides the geometry into irregularly shaped elements, approximating the temperature distribution within each element using piece-wise polynomial functions. The FEM can therefore offer more accurate solutions, particularly for complex geometries, but requires additional computational resources.

Thus, to validate the MATLAB FDM-M, it was compared with an identical 2D geometry FEM in the ANSYS Workbench. The validation process involved assessing the cooling times required to reach −45 °C within the fracture area of the steel wall at different cooling bandwidths. The comparison revealed a perfect match between the cooling times obtained from the MATLAB FDM-M and the ANSYS FEM approach for all bandwidths tested, as shown in Figures 11a and 11b, respectively. This agreement suggests that the FDM-M is a valid and accurate method for analysing transient heat transfer in a specified steel wall geometry. However, it is noted that achieving a perfect match may not always be possible owing to the inherent limitations and assumptions of numerical methods, as well as the complexities and sources of error in the physical system being analysed.

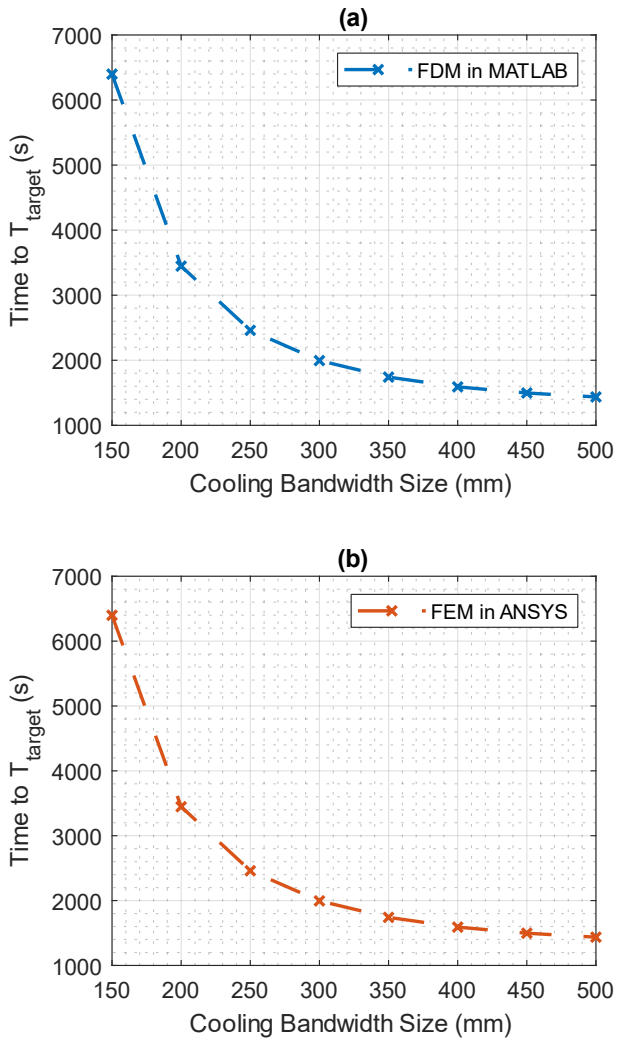

Figure 11. Validation of the cooling times determined for a W_t of 100 mm applying the (a) MATLAB finite difference method model (FDM-M) and (b) ANSYS finite element method (FEM) approaches.

The decision to rely on software-only validation in this study is grounded in several key considerations. More specifically, the complexity and scale of offshore structures, such as medium-carbon steel processing pipes, render physical experimentation under cryogenic conditions both logistically challenging and prohibitively expensive. Setting up such large-scale experiments would require extensive resources, specialised facilities, and extended timelines, indicating their impracticality for routine validation. Moreover, the near-perfect agreement between the MATLAB FDM-M and ANSYS FEM results further demonstrates the accuracy and reliability of the FDM-M for simulating cryogenic cooling processes. This cross-validation with industry-standard software ensures the robustness of the numerical simulations, thereby rendering them suitable for use in real-world applications.

Software simulations also provide a controlled environment where variables such as air velocity, ambient temperature, and cooling surface conditions can be precisely manipulated, something that is difficult to achieve consistently in physical experiments. This flexibility allows for the systematic exploration of a range of ambient conditions in a repeatable and efficient manner, providing a deeper understanding of the cooling processes involved. While experimental data could offer additional validation, the computational methods used in this study are well-established and provide an accurate and efficient means of investigating the effects of ambient conditions on cryogenic cooling times. Future research may incorporate experimental verification in smaller-scale setups, but for the purposes of this study, software validation remains an effective and reliable approach.

4. Discussion

This study explored the behaviour of medium-carbon steel (ISO EN 1.0456, ASTM A333 Gr.6) under cryogenic conditions, with a particular focus on the DBTT. The sharp decrease observed for E_i as the temperature was reduced (see Figure 1), underscores the effectiveness of cryogenic conditions for the low-energy fracturing of medium-carbon steel grades. The FDM-M, developed in MATLAB, proved to be an effective tool for simulating THT processes in medium-carbon steel, allowing for accurate cooling-time predictions and improving the reliability of the simulations.

The study specifically examined the effects of temperature on the E_i value of ISO EN 1.0456 (ASTM A333 Gr.6) medium-carbon steel. The DBTT phase diagram (Figure 1) serves as a crucial reference for low energy fracturing applications, illustrating the relationship between the temperature and E_i. Moreover, the evaluation of the CCCS using liquid nitrogen (LN_2) provided valuable insights into how ambient conditions, such as air velocity and temperature, influence cooling times. The exploration of LN_2 as a cooling medium also revealed important information regarding its thermal properties and its impact on both energy absorption and cooling times in medium-carbon steel. This knowledge is essential for fine-tuning the CCCS to ensure the efficient and low-impact fracturing of medium-carbon steel structures. This study thoroughly analysed the effects of the ambient air velocity, the air temperature, and the cooling medium on the resulting cooling times. The results presented in Figures 6 and 7 underscore the critical influence of these factors in achieving optimal cooling outcomes.

Practical considerations, such as the effects of insulating residues (e.g., crude oil sludge), were also addressed. The results shown in Figure 9 reveal that the presence of insulating residues reduced cooling times by 13.6%, highlighting the importance of accounting for such insulating effects in real-world applications. This is particularly relevant for industrial

decommissioning scenarios where contaminants may be present inside the pipes.

The cooling time calculations, validated against ANSYS Workbench's commercial FEM software, confirmed the reliability of the MATLAB FDM-M approach. The near-perfect match in cooling times between the two methods, as presented in Figures 11a and 11b, underscores the accuracy of the FDM-M model for transient heat transfer analysis. According to Christensen (2023) and Christensen et al. (2024), the MATLAB Finite Difference Method Model (FDM-M) has been shown to hold true for a wide array of low and medium carbon steel grades, further supporting the robustness of the model across various materials within this category. Although this study focused on medium-carbon steel (ISO EN 1.0456), the findings can be cautiously extended to other carbon steel grades due to their shared BCC crystal structures, which exhibit similar embrittlement behaviours at low temperatures.

Moreover, a trade-off between increasing the internal cooling surface area for faster cooling and the associated costs and energy consumption was analysed. While larger cooling surfaces were found to reduce cooling times, they demand a proportional increase in the cooling aid, thereby increasing the overall energy consumption. This balance is crucial for the practical and cost-effective implementation of CCCS in industrial settings.

Moreover, quantitative analysis revealed that for each 2.5 m s−1 increment in the air velocity, cooling times increased by ~11 s for XS specimens and 25 s for XXS specimens. Conversely, the air temperature had a significantly greater impact, with cooling times nearly doubling as the temperature was increased by 40 °C. This result suggests that air temperature plays a more dominant role than air velocity in determining cooling efficiency, thereby rendering temperature control a key focus in optimising cryogenic cooling processes for decommissioning operations.

The findings of this study highlight the significant potential of the CCCS in promoting more sustainable industrial practices, particularly in the context of offshore decommissioning. By substantially reducing cooling times and enhancing energy efficiency, the CCCS aligns with Sustainable Development Goals 9 (Industry, Innovation, and Infrastructure) and 13 (Climate Action), offering a low-impact, energy-efficient alternative to traditional cutting techniques. Additionally, the reduction in operational costs and environmental risks enhances the overall sustainability of the decommissioning process.

5. Conclusions

The research presented in this study, which is based solely on numerical simulations using the finite difference method model (FDM-M) developed in MATLAB, provides valuable insights into the effects of ambient conditions on cryogenic cooling times for medium-carbon steel geometries. No experimental work was conducted; instead, all findings were derived from computational models validated against commercial finite element method (FEM) software. The key findings of this study highlight the measurable impact of the air velocity and the air temperature on the required cooling times. More specifically, increasing the air velocity from 0 to 25 m s−1 led to a 5.7% increase in the cooling time for the XS specimens and a 6.9% increase for the XXS specimens. However, the ambient air temperature had a far more significant effect, with cooling times increasing by 93% for the XS specimens and 106% for the XXS specimens when the ambient temperature was increased from −10 to 30 °C. This demonstrates that while air velocity plays a role, temperature control is the more influential factor in optimising the cooling efficiency. Moreover, a detailed analysis revealed that with each 2.5 m s−1 increment in the air velocity, the cooling times increased by 11 s for the XS specimens and 25 s for the XXS specimens. In contrast, a 40 °C increase in the air temperature nearly doubled the cooling time, underscoring the critical importance of temperature management in cryogenic cooling processes for offshore decommissioning. The cooling efficiency was also closely linked to the cooling internal surface area exposed to the cryogenic agent. More specifically, a larger internal surface area enabled more effective cooling, but required a proportional increase in the cooling aid, leading to a higher energy consumption. This trade-off emphasises the need for a balanced approach, particularly when considering practical and energy-efficient applications of the CCCS. It is important to note that while these findings are relevant to medium-carbon steel (ISO EN 1.0456, ASTM A333 Gr.6), the conclusions should not be overgeneralised to all carbon steel grades. Further research is therefore necessary to confirm the applicability of these results across a wider range of steel compositions. Moreover, to enhance the performance of the CCCS, future research should explore strategies for reducing energy demands associated with larger cooling surfaces. Potential innovations, such as integrating heat elements into the process, may help offset energy consumption while maintaining an appropriate cooling precision. Furthermore, a comprehensive analysis of the environmental and sustainability impacts of the CCCS should be a key focus of future investigations. Overall, this research provides a robust foundation for understanding the complexities of cryogenic cooling in medium-carbon steel decommissioning. The challenges identified open new avenues for further research aimed at refining the CCCS, optimising its parameters, and exploring broader industrial applications. The integration of theoretical and practical insights will also be essential for advancing sustainable and energy-efficient fracturing and cutting technologies in an industrial setting.

Authorship contribution statement

Kenneth Bisgaard Christensen, Alireza Maheri, and M. Amir Saddiq jointly contributed to the conceptualization of mathematical models and research methodology. Kenneth Bisgaard Christensen took the lead in implementing the methods, in addition to designing and conducting numerical experiments, interpreting the results, and drafting the manuscript. Alireza Maheri and M. Amir Saddiq played a significant role in editing and critically reviewing the final manuscript. All authors provided final approval for the publication of this research.

Declaration of competing interest

Kenneth Bisgaard Christensen, Alireza Maheri, and M. Amir Saddiq jointly contributed to the conceptualisation of the mathematical models and the research methodology. Kenneth Bisgaard Christensen took the lead in implementing the methods, in addition to designing and conducting the numerical experiments, interpreting the results, and drafting the manuscript. Alireza Maheri and M. Amir Saddiq played significant roles in editing and critically reviewing the final manuscript. All authors provided their final approval for the publication of this research.

Data availability statement

The data used in this study are available upon request. Researchers or individuals interested in accessing data may contact the corresponding author for further information. We are committed to promoting transparency and facilitating access to data for scientific and research purposes.

Acknowledgements

The research presented in this paper is partially derived from the work conducted within the framework of the project titled 'Eco-innovative concepts for the end of the offshore wind energy farm lifecycle' (DecomTools). We gratefully acknowledge the financial support provided by the European Commission through the Interreg VB North Sea Region Programme under Project No. 20180305091606 as well as the work performed by the Scottish Research Partnership in Engineering (SRPe) for Advanced Manufacturing, researching a competitive and sustainable cutting solution for the offshore industry under Grant No. NMIS-IDP/018. This funding has been instrumental in enabling our research efforts and contributions to the field of offshore wind energy and material behavior under low temperatures.

References

1 Fowler A M, Macreadie P I, Jones D O B and Booth D J 2014 A multi-criteria decision approach to decommissioning of offshore oil and gas infrastructure *Ocean Coast. Manag.* **87** 20. doi: 10.1016/j.ocecoaman.2013.10.019

2 Sommer B, Fowler A M, Macreadie P I, Palandro D A, Aziz A C and Booth D J 2019 Decommissioning of offshore oil and gas structures – Environmental opportunities and challenges *Sci. Total Environ.* **658** 973. doi: 10.1016/j.scitotenv.2018.12.193

3 Ekins P, Vanner R and Firebrace J 2006 Decommissioning of offshore oil and gas facilities: A comparative assessment of different scenarios *J. Environ. Manage.* **79** 420. doi: 10.1016/j.jenvman.2005.08.023

4 Sandal K, Verbart A and Stolpe M 2018 Conceptual jacket design by structural optimization *Wind Energy* **21** 1423. doi:10.1002/we.2264

5 Nguyen C T and Oterkus S 2019 Peridynamics formulation for beam structures to predict damage in offshore structures *Ocean Eng.* **173** 244

6 Rao B N and Acharya A R 2016 Fracture behavior of a high strength medium carbon low alloy steel *Eng. Fract. Mech.* **53** 303

7 Beinke T, Ait Alla A and Freitag M 2018 Decommissioning of offshore wind farms *International Conference on Dynamics in Logistics* (Cham: Springer) p 216–222

8 Hsu C-Y, Liang C-C, Teng T-L and Nguyen A-T 2013 A numerical study on high-speed water jet impact *Ocean Eng.* **72** 98. doi: 10.1016/j.oceaneng.2013.06.012

9 Rouse S, Hayes P, Davies I M and Wilding T A 2018 Offshore pipeline decommissioning: Scale and context *Mar. Pollut. Bull.* **129** 241. doi: 10.1016/j.marpolbul.2018.02.041

10 Vidal P C J, González M O A, Vasconcelos R M, Melo D C, Ferreira P O, Sampaio P G V and Silva D R 2022 Decommissioning of offshore oil and gas platforms: A systematic literature review of factors involved in the process *Ocean Eng.* **255** 111428. doi: 10.1016/j.oceaneng.2022.111428

11 Chandler J, White D, Techera E J, Gourvenec S and Draper S 2017 Engineering and legal considerations for decommissioning of offshore oil and gas infrastructure in Australia *Ocean Eng.* **131** 338. doi: 10.1016/j.oceaneng.2016.12.030

12 Yi S, Liu X L, Li Q and Zhang Z 2021 Analysis of crack causes and effects of the A333 low carbon pipeline steel after thermite welding *Eng. Fail. Anal.* **130** 105774

13 Bisgaard Christensen K, Maheri A, Saddiq M A and Jalili S 2024. *A study on the potential of cryogenic cooling and cutting technique in reducing the decommissioning cost of offshore wind turbines*. Preprint SSRN.. doi:10.2139/ssrn.477398

14 Capobianco N, Basile V, Loia F and Vona R 2021 Toward a sustainable decommissioning of offshore platforms in the oil and gas industry: A PESTLE analysis *Sustainability* **13** 6266

15 ASTM International 2018 ASTM A333/*A333M-16, standard specification for seamless and welded steel pipe for low-temperature service and other applications with required notch toughness* (West Conshohocken, PA: ASTM International)

16 Bisgaard Christensen K B, Jalili S and Maheri A 2022. A comparative assessment of cutting techniques for offshore energy structures 7th *International Conference on* Environment Friendly Energies *and* Applications *(EFEA)* (vol 2022). doi: 10.1109/EFEA56675.2022.10063821

17 Brozek M 2017 Steel cutting using abrasive water jet *Eng. Rural Dev.* 75

18 Wilkinson W B, Bakke T, Clauss G F, Clements R, Dover W D, Rullkötter J and Shepherd J G 2016 Decommissioning of large offshore structures – The role of an independent review group (IRG) *Ocean Eng.* **113** 11. doi: 10.1016/j.oceaneng.2015.12.031

19 Devi V G, Kumar S R, Yadav D, Lathiya P and Sircar A 2020 Design and thermal fluid structure interaction analysis of liquid nitrogen cryostat of cryogenic molecular sieve bed adsorber for hydrogen isotopes removal system *Fusion Eng. Des.* **151** 111376

20 Jha A R 2006 *Cryogenic technology and applications* (Oxford: Butterworth-Heinemann)

21 Leachman, J.W. et al., 2017. Thermodynamic properties of cryogenic fluids. Cham: Springer.

22 Timmerhaus K D and Reed R P 2007 *Cryogenic Engineering: Fifty years of progress* (New York, NY: Springer)

23 Phelps C 2019 *Carbon steel: Microstructure, mechanical properties and applications* (Nova Science Publishers Inc)

24 Barron R and Nellis G 2016 *Cryogenic heat transfer*, 2nd edn (Boca Raton, FL: CRC Press)

25 Breen B P and Westwater J W 1962 Effect of diameter of horizontal tubes on film boiling heat transfer *Chem. Eng. Prog.* **58** 67

26 Dominique F, André P and Zaoui A 2013 *Mechanical behaviour of materials* (Dordrecht: Springer)

27 Rana M D, Doty W D, Yukawa S and Zawierucha R 2001 Fracture toughness requirements for ASME Section VIII Vessels for Temperatures Colder Than 77K *J. Press. Vessel Technol.* **123** 332. doi: 10.1115/1.1376125

28 Edejer M P and Thodos G 1967 Vapor pressures of liquid nitrogen between the triple and critical points *J. Chem. Eng. Data* **12** 206

29 NIST office of data and informatics, n.d. nitrogen, https://webbook.nist.gov/cgi/cbook.cgi?ID=C7727379&Mask=4. (Accessed 22 Jan 2024)

30 Arntsen G R 2020. *Stål Håndbogen. Kbh: Kvalitets-Instituttet*

31 Bisgaard Christensen K 2023 *On the Application of Cryogenic Cooling and Cutting for Offshore Energy Structures*. Unpublished PhD Thesis (University of Aberdeen)

32 Harvey P D 2011 *Engineering properties of steel* (Metals Park, OH: American Society for Metals International)

33 ASTM International 2018. *ASTM E23-18: Standard test methods for notched bar impact testing of metallic materials* (ASTM International)

34 Make it 2020 *MakeItFrom.com*, https://www.makeitfrom.com/material-properties/EN-1.0456-E275K2-Non-Alloy-Steel. (Accessed 22 Jan 2024)
NIST office of data and informatics, n.d. nitrogen, https://webbook.nist.gov/cgi/cbook.cgi?ID=C7727379&Mask=4. (Accessed 22 Jan 2024)

35 Krex H E 2004 *Maskin Ståbi. Kbh* (Nyt Teknisk Forlag)

36 Sun M and Packer J A 2014 Charpy V-notch impact toughness of cold-formed rectangular hollow sections *J. Constr. Steel Res.* **97** 114. doi: 10.1016/j.jcsr.2014.02.005

37 Engineering toolbox 2022 *Convective heat transfer. Engineering toolbox*, https://www.engineeringtoolbox.com/convective-heat-transfer-d_430.html. (Accessed 22 Jan 2024)

38 Çengel Y A 2004 *Heat transfer: A practical approach* (Boston, MA: McGraw-Hill)

39 ASTM International 2004 *ASME B36.10M-2004, an American national standard for seamless wrought steel pipe* (3 Park Avenue, NY: *The American Society of Mechanical Engineering*) p 10016-5990

40 Baru A, Efzan M N, Kesahvanveraragu S and Emerson J A 2014 *Microstructural characterization and hardness properties of A333 Grade 6 low carbon steel in offshore platform pipelines*